Kovove Mater. 49 2011 417–426
DOI: 10.4149/km_2011_6_417

The influence of PWHT regime on microstructure and creep rupture behaviour of dissimilar T92/TP316H ferritic/austenitic welded joints with Ni-based filler metal

L. Falat[1]*, A. Výrostková[1], M. Svoboda[2], O. Milkovič[3]

[1] *Institute of Materials Research, Slovak Academy of Sciences, Watsonova 47, 040 01 Košice, Slovak Republic*
[2] *Institute of Physics of Materials, Academy of Sciences of the Czech Republic, Žižkova 22, 616 62 Brno, Czech Republic*
[3] *Technical University of Košice, Faculty of Metallurgy, Department of Materials Science, Park Komenského 11, 042 00 Košice, Slovak Republic*

Received 27 July 2011, received in revised form 3 August 2011, accepted 16 August 2011

Abstract

In this paper the dissimilar welded joints between the ferritic (tempered martensitic) steel T92 and the non-stabilised austenitic steel TP316H were investigated in terms of microstructure and creep rupture behaviour characterisation. The welded joints were prepared by the TIG method using the Ni-based filler metal Nirod 600 (Inconel-type). After the welding, the individual weldments were subjected to the two different regimes of post-weld heat treatment (PWHT), either the "classical" PWHT (i.e. subcritical tempering – below A_{c1} temperature) or the so-called "full" PWHT including the re-normalisation. The use of "classical" PWHT preserved microstructural gradient in the ferritic steel heat-affected zone (HAZ), which led to a premature creep failure by the "type IV cracking" mode. In contrast, the application of "full" PWHT eliminated the critical HAZ region of T92 steel and changed the creep failure mode to the "interfacial cracking" between the ferritic steel and the Ni-based weld metal. Consequently, this suppression of the "type IV cracking" failure led to a significant creep life increase of the studied ferritic/austenitic welded joints.

K e y w o r d s: dissimilar weldment T92/TP316H, post-weld heat treatment (PWHT), microstructure, creep, type IV cracking, interfacial cracking

1. Introduction

Dissimilar weldments of creep-resistant steels are commonly used in a boiler system of fossil-fired power plants [1, 2]. Whereas in a primary part of supercritical steam boiler the Cr-Mo ferritic steels are used for water evaporators (membrane water walls) and steam headers [3, 4], in the terminal part of superheaters and reheaters the Cr-Ni austenitic steels are employed [5, 6].

The first produced ferritic/austenitic (α/γ) weldments were manufactured by fusion welding using the filler materials based on austenitic steels [1, 2]. The most serious problem in these welds was associated with carbon migration from ferrite to austenite driven by carbon activity gradient [2, 7–9]. To overcome this problem, the alternative nickel-based welding consumables of Inconel-type have been introduced. The Ni-based fillers possess low carbon solubility, so they act like a carbon diffusion barrier and hence the carbon depletion at the ferritic side of the dissimilar α/γ weldment is considerably suppressed [2, 7].

The majority of published studies on dissimilar α/γ weldments with Ni-based filler metal were performed on the welds with 2.25Cr-1Mo ferritic steel base material [10–16]. These studies were focused mainly on microstructure evolution of either service-exposed or laboratory heat-treated weldments. However, the literature information on the α/γ welds with advanced high Cr ferritic steels is very limited. For in-

*Corresponding author: tel.: +421-55-792-2447; fax: +421-55-792-2408; e-mail address: lfalat@imr.saske.sk

Table 1. Chemical composition (wt.%) of the base steels

Steel	C	N	Si	Mn	P	S	Cr	Mo	W	B	Ni	Al	V	Nb	Fe
T92	0.11	0.056	0.38	0.49	0.019	0.002	9.08	0.31	1.57	0.0023	0.33	0.014	0.2	0.069	Balance
TP316H	0.052	–	0.51	1.77	0.031	0.006	16.76	2.05	–	–	11.13	–	–	–	Balance

Table 2. Chemical composition (wt.%) of the Ni-based filler metal

Alloy	C	Si	Mn	P	S	Cr	Fe	Nb	Ni
Nirod 600	0.05	0.3	3.0	0.03	0.015	20.0	2.0	2.0	Balance

stance, the studies [17, 18] deal with thermal cycling experiments on the dissimilar α/γ welds with P91 ferritic steel but the information about their creep behaviour is not available. Moreover, there is a lack of any comparative studies about the influence of PWHT conditions on microstructure and creep performance of these welds.

Generally, the weldments of high Cr ferritic steels require the application of PWHT in order to relieve residual stresses and stabilise the microstructure [3, 19, 20]. The "classical" PWHT of these welds consists of subcritical tempering (i.e. below A_{c1} temperature), typically in the range from 720 to 760 ℃ [3, 19]. It is well-known that the "classical" PWHT decreases the hardness of a welded joint and improves its toughness [3, 21–23]. However, the remaining problem during creep exposure of these weldments is their premature failure by the "type IV cracking" mode, i.e. the failure within the fine-grained intercritical HAZ region [24–28]. Albert et al. [24] reported that this failure type cannot be avoided by any variation in subcritical ("classical") PWHT regime. Some authors [29–31] suggest that the only way to avoid "type IV cracking" in the ferritic welds is their complete re-normalisation.

In the case of dissimilar α/γ weldments the PWHT conditions are generally proposed with respect to the ferritic steel of the joint, according to the "classical" PWHT regime. The relevant literature data focusing on the possibility of application of "full" PWHT (re-normalisation followed by subcritical tempering) on the α/γ welds are missing. Therefore, a present study was undertaken to investigate the influence of different PWHT regimes (the "classical" and the "full" PWHT) on microstructure and creep rupture behaviour of dissimilar T92/TP316H ferritic/austenitic welded joints.

2. Experimental procedure

The tubes of dissimilar steels T92 and TP316H (38 mm outer diameter, 5.6 mm wall thickness) were circumferentially welded by the TIG method using the Ni-based filler metal Nirod 600. Welding parameters were the following: welding current 70–110 A, voltage 12–17 V, and heat input 9–12 kJ cm^{-1}. The diameter of TIG electrode was 2.4 mm and the negative polarity on the electrode was used. The chemical compositions of the materials used for the production of the weldments are given in Tables 1 and 2.

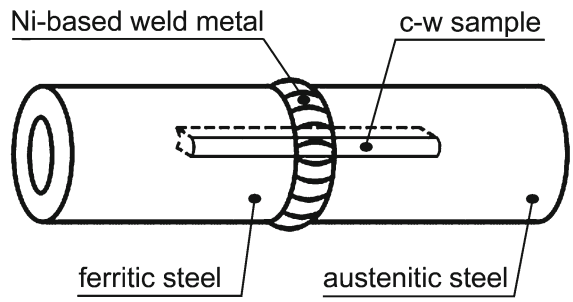

Fig. 1. Schematic cross-weld (c-w) sampling.

After the welding, two different PWHT regimes were applied to the first and second series of the produced T92/TP316H welded joints, respectively. The "classical" PWHT regime consisted of subcritical tempering (i.e. below A_{c1} temperature) at 760 ℃/60 min, followed by furnace cooling down to the room temperature. The second series of the welded joints was subjected to the "full" PWHT including the re-normalisation (1060 ℃/15 min/water quench) and subsequent subcritical tempering.

For all following experiments the cross-weld (c-w) samples were used. The sectioning of the tubular T92/TP316H welded joint to the c-w blocks is schematically shown in Fig. 1. One of the cut blocks was used for the metallographic examination. The other blocks were used for the machining of round tensile samples (4 mm body diameter, 40 mm gauge length, M6 head thread) for the creep rupture tests.

Metallographic analyses involved light microscopy (LM), scanning electron microscopy (SEM) linked with energy dispersive X-ray analysis (EDX), and transmission electron microscopy (TEM). For LM and SEM observations the samples were ground, polished

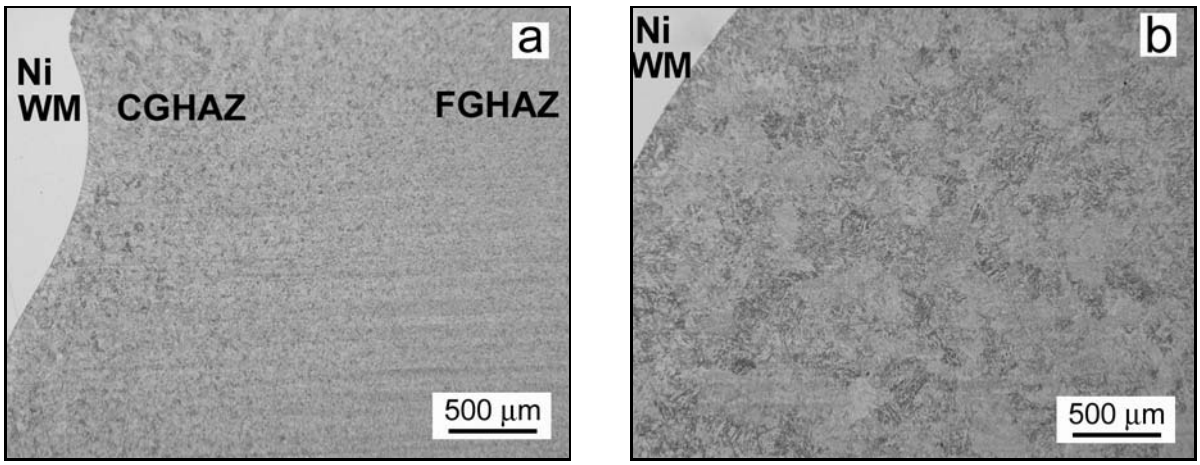

Fig. 2. Microstructure of the ferritic part of the T92/TP316H weld joint after the "classical" PWHT (a) and after the "full" PWHT (b).

Table 3. Etchants used for the etching of dissimilar materials

Material	composition of etching solution
T92, TP316H	120 ml CH_3COOH, 20 ml HCl, 3 g picric acid, 144 ml CH_3OH
Nirod 600	5 ml HF, 10 ml HNO_3, 85 ml H_2O

and etched. For the etching of dissimilar materials the different etching solutions were used (Table 3).

For the TEM observations thin foils were prepared by mechanical grinding and polishing, and electrolytic thinning in the solution: 70 ml $HClO_4$ + 930 ml CH_3OH, at temperature −35 ℃ and voltage 20–25 V.

3. Results and discussion

3.1. The influence of PWHT regime on microstructure

Figures 2–5 show the light optical microstructures of different regions of the studied T92/TP316H welded joint in two different PWHT states. In Fig. 2a,b the microstructure of the ferritic (T92) region next to the Ni-based weld metal (Ni WM) is shown for the "classical" as well as for the "full" PWHT state, respectively. After the "classical" PWHT the T92 microstructure exhibits a typical HAZ region consisting of its coarse-grained (CGHAZ) and fine-grained (FGHAZ) part (Fig. 2a). On the other hand, after the "full" PWHT the T92 microstructure is free of the HAZ region (Fig. 2b) as a result of transformation processes (re-austenitisation and back on-cooling martensite formation) during this PWHT regime. In addition, the "fully" post-weld heat treated microstructure is much coarser than the CGHAZ microstructure corresponding to the "classical" PWHT (see details in Fig. 3a,b). The coarser T92 microstructure after the "full" PWHT originates from the coarsening of prior austenite grains during the re-austenitisation period of this heat treatment.

In Fig. 4a,b the microstructures of the austenitic (TP316H) region next to the Ni WM are shown for the "classical" as well as for the "full" PWHT state, respectively. In contrast to the ferritic part of the weld joint, the microstructures of the austenitic part are only slightly affected by the PWHT conditions with respect to the grain size. After the "full" PWHT only some individual grains of the TP316H steel are coarsened (Fig. 4b), compared to the microstructure after the "classical" PWHT (Fig. 4a). Since the microstructures of the ferritic creep-resistant steels (including T92 steel) as well as the austenitic stainless steels (type AISI 316) have been widely studied by many other authors [32–40], no further detailed microstructural and/or phase analyses were carried out here on these steels.

The microstructures of the Ni WM Nirod 600 close to the interface with T92 steel are documented for the both studied PWHT states in Fig. 5. (After the selective etching of the Ni WM, the T92 material becomes over-etched and hence appears fully dark.) The microstructures of Ni WM after the both PWHT regimes are very heterogeneous with respect to the size, morphology and distribution of grains and precipitates. In the "classical" PWHT state (Fig. 5a) the microstructure contains well-preserved solidification grain boundaries as well as sub-grain boundaries (in this case – dendritic cell boundaries). To the contrary, after the "full" PWHT (Fig. 5b) the microstructure of Ni WM contains mostly migrated grain boundaries as a result of their intensive migration during the heat treatment. The size of precipitates in the "fully" heat treated microstructure (Fig. 5b) is signi-

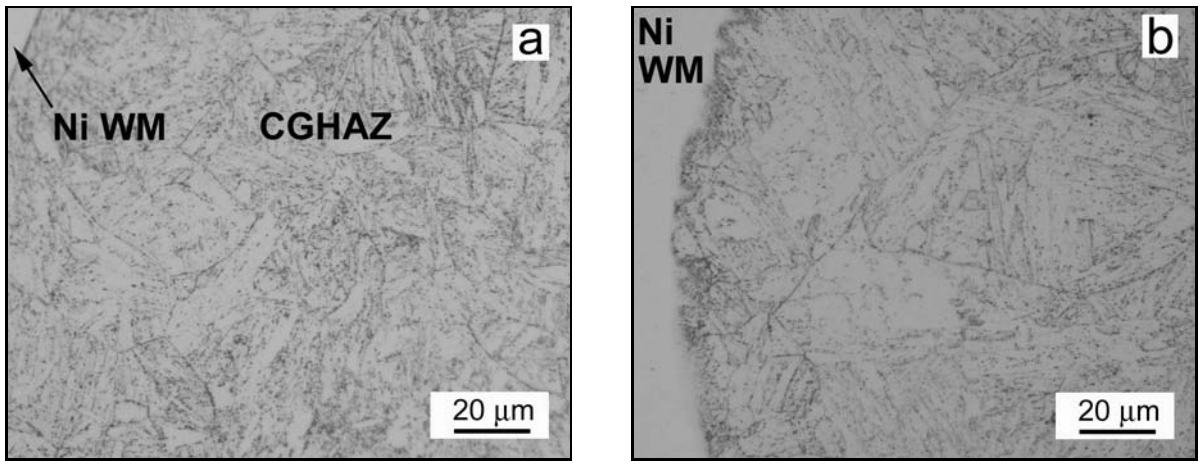

Fig. 3. Detailed microstructures of the ferritic part of the T92/TP316H weld joint after the "classical" PWHT (a) and after the "full" PWHT (b).

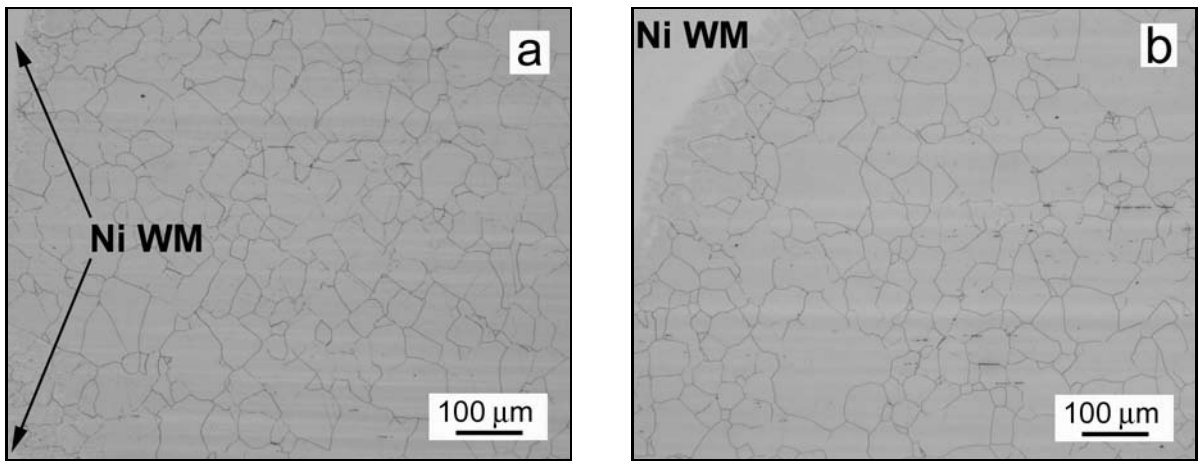

Fig. 4. Microstructures of the austenitic part of the T92/TP316H weld joint after the "classical" PWHT (a) and after the "full" PWHT (b).

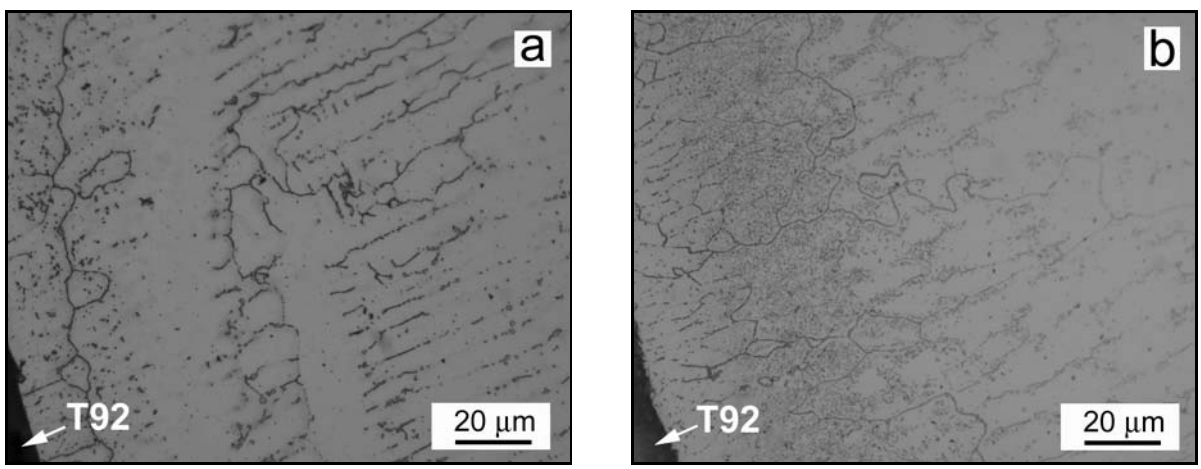

Fig. 5. Microstructures of the Ni WM Nirod 600 close to the interface with T92 steel after the "classical" PWHT (a) and after the "full" PWHT (b).

ficantly finer compared to the "classical" PWHT state (Fig. 5a). This refinement of the precipitates is given by their dissolution during the re-normalisation and back re-precipitation during the subsequent tempering. The microstructures in Fig. 5 contain intergranular as well as intragranular precipitates with different

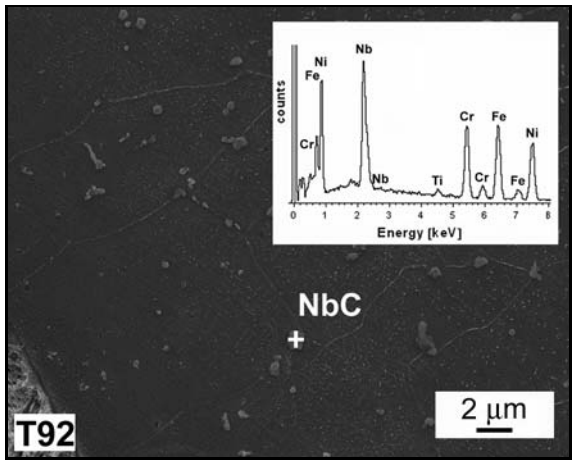

Fig. 6. Blocky Nb-rich precipitate in Nirod 600 weld metal and its corresponding EDX spectrum.

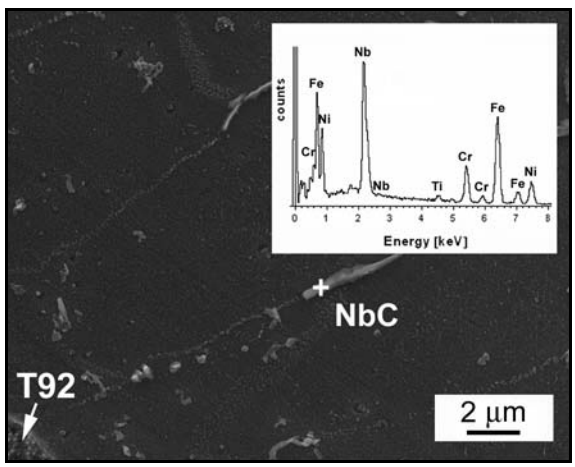

Fig. 7. Intergranular Nb-rich precipitate in Nirod 600 weld metal and its corresponding EDX spectrum.

morphologies. The precipitates are either blocky or they form more-less continuous structures along the grain boundaries. By means of EDX analyses both these precipitate types were found to be rich in Nb (Figs. 6 and 7). With respect to the overall chemical composition of the Nirod 600 weld metal (Table 2) the precipitates are likely the NbC carbides. Indeed, the occurrence of these precipitates was also reported by Ramirez and Lippold [41] in their study on the filler metal "FM 82" with the chemical composition very similar to that of the Nirod 600 weld metal. In addition, Jonšta et al. [42] also observed these precipitates in another "Inconel-type" Ni-based alloy. The agglomerations of fine intragranular precipitates in Nirod 600 weld metal were analysed by EDX and selected area electron diffraction (SAED) on carbon extraction replicas in TEM. These fine particles were also found to be the NbC carbides with face-centered cubic (f.c.c.) crystal structure (Fig. 8).

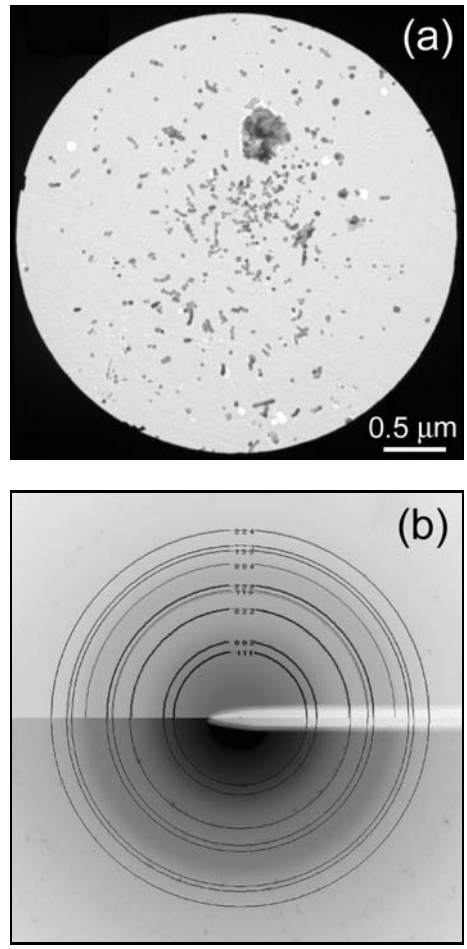

Fig. 8. Agglomerations of fine intragranular NbC precipitates in Nirod 600 weld metal (a) and their corresponding SAED pattern (b).

3.2. The influence of PWHT regime on creep rupture behaviour

In Fig. 9 the stress dependences of the creep life (time-to-fracture) of the studied welded joints are shown at two temperatures (625 and 650 ℃) for the "classical" and the "full" PWHT state. As expected, with decreasing stress and/or temperature the creep life for the both PWHT states increases. However, it is shown that for all stresses at a given temperature the creep life of the weldments after the "full" PWHT is always higher than that after the "classical" PWHT. In addition, with decreasing applied stress the difference in creep life between the "classical" and "full" PWHT state increases. This creep life increase is indicated in Fig. 9 by arrows. These results of creep rupture tests clearly indicate a strong potential of the "full" PWHT for the increase of creep life of dissimilar ferritic/austenitic welded joints.

In Fig. 10 the influence of creep conditions and PWHT regime on the failure mode of the studied weld-

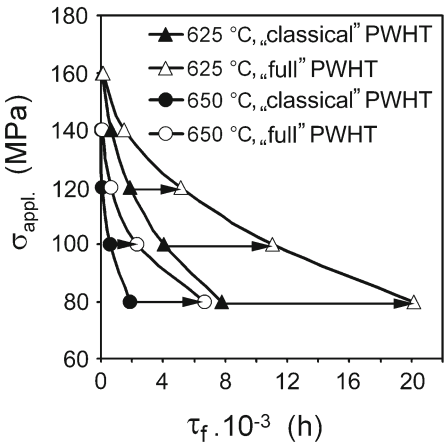

Fig. 9. Creep life of T92/TP316H weld joint in dependence of applied stress, testing temperature and PWHT regime.

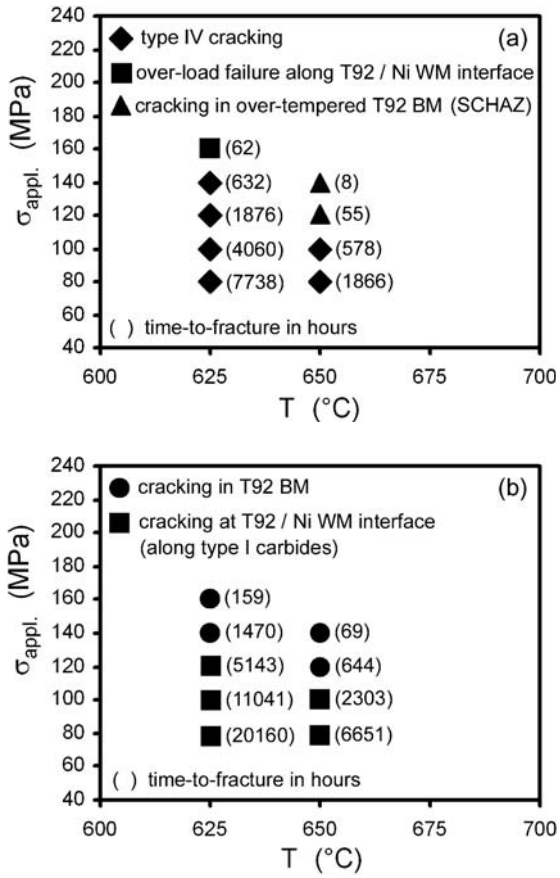

Fig. 10. Influence of creep conditions on failure mode of T92/TP316H weld joint after the "classical" PWHT (a) and after the "full" PWHT (b).

ments is shown. It is obvious that the long-term creep failure mode of the studied weld joints is either the "type IV cracking" or the "cracking at T92/Ni WM interface" for the "classical" and the "full" PWHT state, respectively.

Figure 11 documents a profile view on the as-crept microstructures beneath the creep fracture surfaces after the "type IV cracking" failure. The failure typically occurs within the fine-grained region of intercritical heat-affected zone (ICHAZ).

A detailed view in Fig. 12 reveals an important role of coarsened precipitates on the intergranular character of this failure type. The different types of precipitates were discriminated by the BSE contrast in the SEM image (Fig. 12b).

The interfacial creep failure by "cracking at T92/Ni WM interface" is documented in Fig. 13. The coalesced creep cavities and cracks are clearly visible along the interface. The detailed SEM-image of interfacial T92/Ni WM microstructure is shown in Fig. 14. It reveals an intensive precipitation in T92 steel at the location close and parallel to the T92/Ni WM interface. This morphological arrangement of the interfacial precipitates was referred to as "type I carbides" in [12, 13]. From Fig. 14 it is obvious that the interfacial creep damage is caused by a progressive growth and inter-linkage of the interfacial precipitates which act like crack nucleation sites. Thus, decohesion along the "type I carbides" is likely to be the controlling

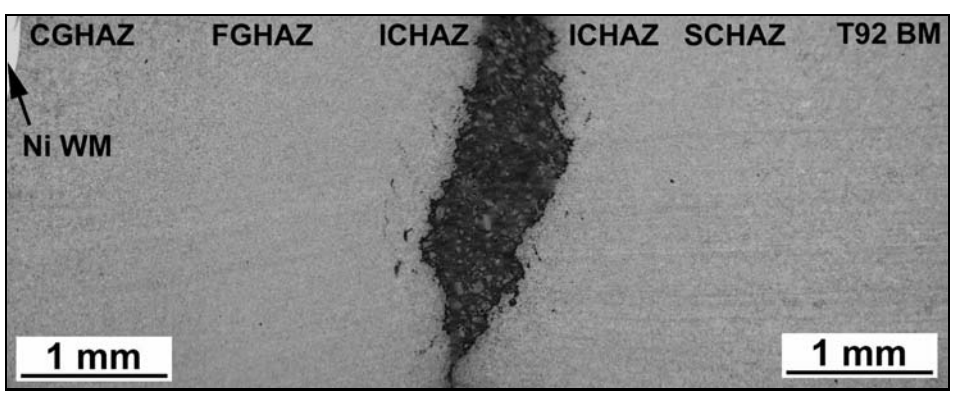

Fig. 11. Light optical microstructures of two counter-parts of the "classically" heat treated weld joint ruptured by "type IV cracking" after 4060 h at 625 °C/100 MPa.

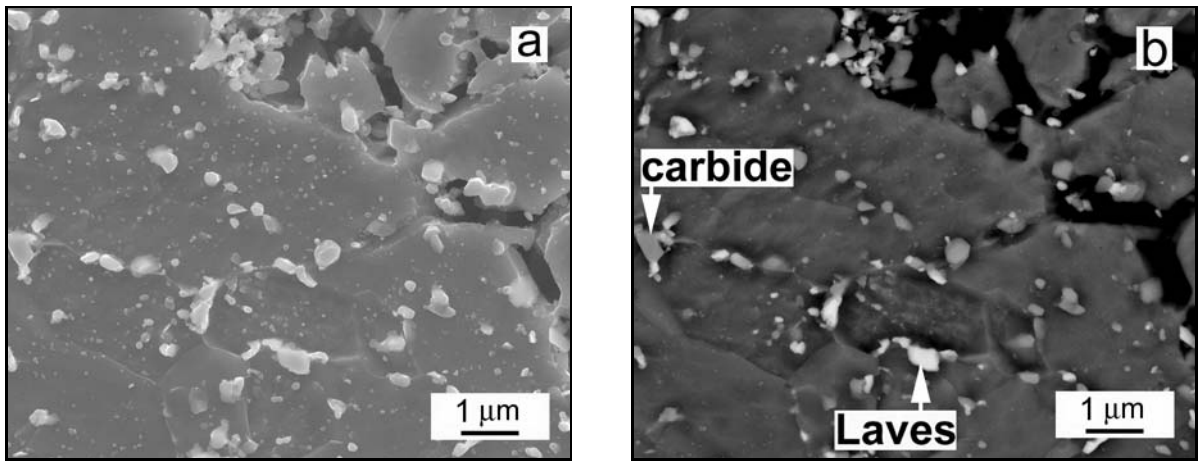

Fig. 12. SEM microstructures of the ICHAZ visualised by the contrast of secondary electrons (a) and back-scattered electrons (b).

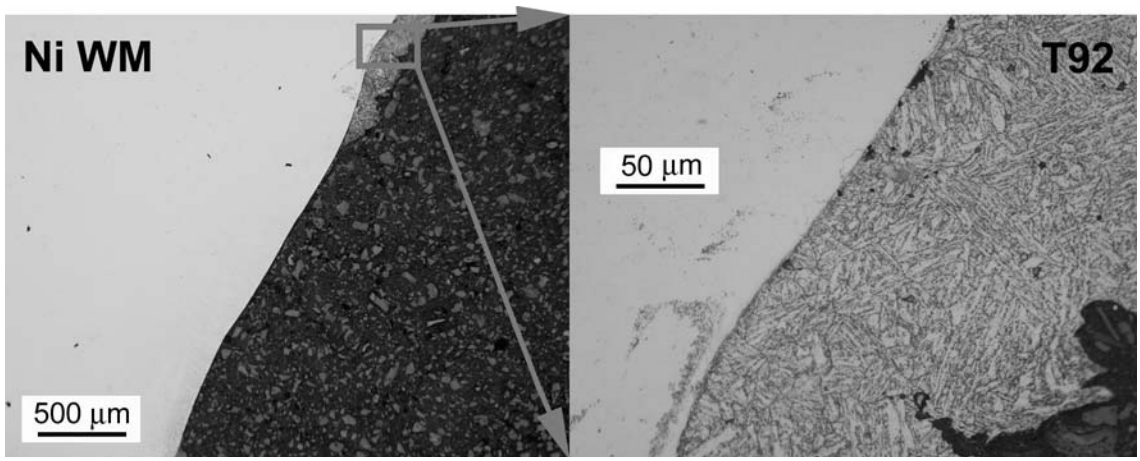

Fig. 13. Failure by "cracking at T92/Ni WM interface" of the "fully" heat treated weld-joint ruptured after 5143 h at 625 °C/120 MPa.

failure mechanism of creep fracture in this case. The formation of interfacial precipitates in different types of dissimilar welds was observed also by many other authors and it was found to be closely related to the redistribution of alloying elements across the weld metal interface [6–9, 11–13, 43–45].

The substructure of ferritic (T92) regions of the investigated T92/TP316H welded joints was characterised by TEM (Fig. 15). The TEM observations were carried out on the as-crept samples with comparable creep exposure corresponding to the both PWHT states. The sampling was always carried out at the location beneath creep fracture. Thus, in the case of "classically" heat treated welded joint the ICHAZ region was investigated (Fig. 15a), whereas in the case of "fully" heat treated weldment the TEM observation was performed in the region close to the T92/Ni WM interface (Fig. 15b). The substructure of T92 ICHAZ after 4060 h of creep at 625 °C/100 MPa contains fully recrystallized polygonal grains with coarse precipit-

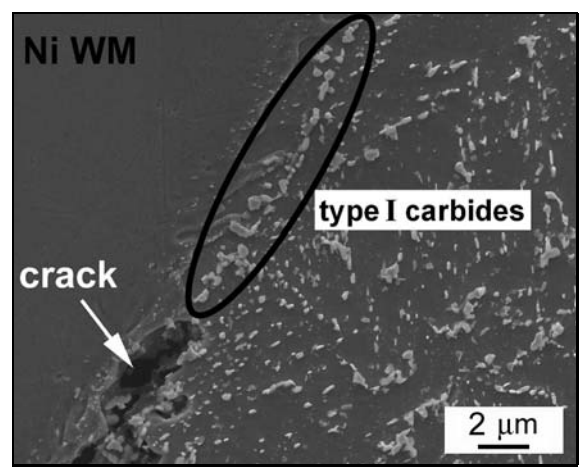

Fig. 14. Detailed SEM-image of interfacial T92/Ni WM microstructure revealing the inter-linkage of interfacial precipitates ("type I carbides") and its relation to the interfacial crack formation.

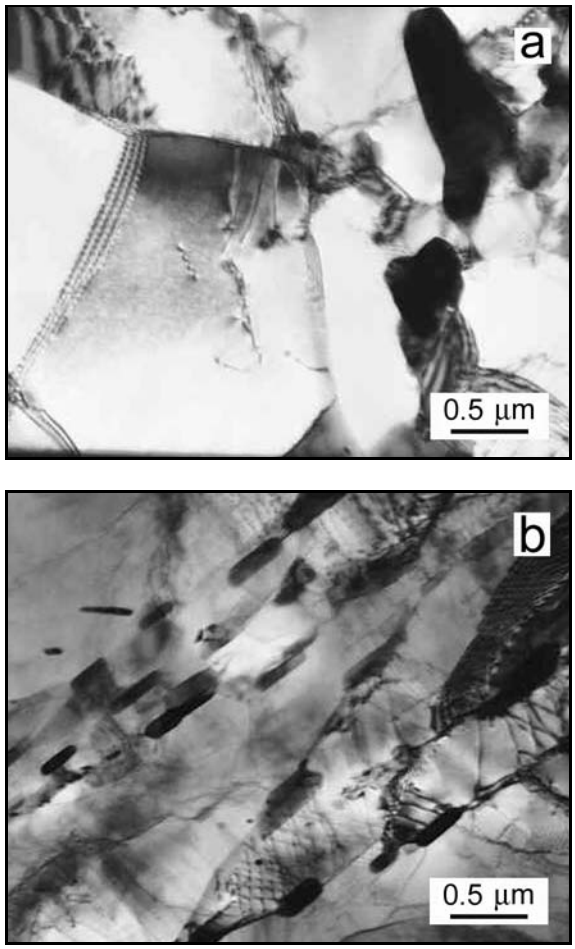

Fig. 15. Substructure of T92 material: (a) ICHAZ region of the "classically" heat treated weld-joint ruptured by "type IV cracking" failure after 4060 h of creep test at 625 ℃/100 MPa; (b) region next to the T92/Ni WM interface of the "fully" heat treated weld-joint ruptured by "cracking at T92/Ni WM interface" after 5143 h of creep test at 625 ℃/120 MPa.

ates (Fig. 15a). In contrast, the substructure of T92 region close to the T92/Ni WM interface still contains laths and relatively finer precipitates (Fig. 15b) even after 5143 h of creep at 625 ℃/120 MPa. The described substructural differences can be directly related to the differences in creep resistance of the studied welded joint in different PWHT states. Thus, the elimination of the T92 ICHAZ region by the "full" PWHT eliminates the "type IV cracking" failure and significantly improves the creep resistance of the T92/TP316H weldment.

4. Summary and conclusions

In this study the effects of different PWHT regimes on microstructure and creep rupture behaviour of the ferritic/austenitic T92/TP316H welded joints were investigated. From the obtained results the following conclusions could be drawn:

– The microstructure of the ferritic steel (T92) of the studied α/γ welds close to the Ni-based weld metal (Nirod 600) exhibits after the "classical" (subcritical) PWHT a typical HAZ region consisting of its coarse-grained and fine-grained part. To the contrary, after the "full" (re-normalised and tempered) PWHT the microstructure of this part of the weldment is markedly coarsened and the original HAZ region is totally eliminated.

– The microstructure of the austenitic steel (TP316H) is only slightly affected by the PWHT conditions.

– In contrast to the microstructure of Nirod 600 in the "classical" PWHT state, its microstructure after the "full" PWHT is significantly affected by the grain boundary migration and the re-precipitation processes.

– The creep rupture behaviour of the investigated α/γ welded joints is controlled by their ferritic part. In dependence of PWHT regime and creep conditions used, several types of creep failure modes were identified. To-the-date results indicate that the long-term creep failure modes are the "type IV cracking" and the "cracking at T92/Ni WM interface" for the welds after the "classical" and the "full" PWHT, respectively.

– The creep-resistance (creep life) of the welded joints after the "full" PWHT is significantly higher than that of the welds after the "classical" PWHT. The crucial reason for this creep life increase is apparently the elimination of the "type IV cracking" failure by the elimination of the fine-grained T92 ICHAZ region after the "full" PWHT. These findings clearly indicate a strong potential of the "full" PWHT for the increase of long-term operation of power plants. However, there is a need to perform the creep tests with much longer durations – about 30 000 h and more (i.e. at the more realistic creep conditions approaching the real operating conditions) in order to verify the obtained tendencies in creep-rupture behaviour and to perform reliable creep strength predictions.

Acknowledgements

The present work was supported by the Slovak Scientific Grant Agency – VEGA under the Grant No. 2/0128/10. The experimental dissimilar welded joints were prepared by the company SES, a.s. Tlmače, Slovak Republic. The authors are grateful to assoc. Prof. Dr. Jozef Pecha (currently at: Energoinvest, a.s. Mochovce, Slovak Republic) for helpful discussions.

References

[1] LUNDIN, C. D.: Weld. J., *61*, 1982, p. 58.

[2] BHADURI, A. K.—VENKADESAN, S.—RODRIGUEZ, P.—MUKUNDA, P. G.: Int. J. Press. Vessels Pip., *58*, 1994, p. 251. http://dx.doi.org/10.1016/0308-0161(94)90061-2
[3] PECHA, J.: Zváranie moderných žiarupevných ocelí pre energetické zariadenia. Bratislava, Slovenská Technická Univerzita 2007 (in Slovak).
[4] ZIFČÁK, P.—BRZIAK, P.—BALOG, M.—BOŠANSKÝ, J.—SRNKA, M.: Acta Metallurgica Slovaca, *14*, 2008, p. 196.
[5] SIREESHA, M.—SHANKAR, V.—ALBERT, S. K.—SUNDARESAN, S.: Mater. Sci. Eng., *A292*, 2000, p. 74. http://dx.doi.org/10.1016/S0921-5093(00)00969-2
[6] BUCHKREMER, H. P.—ENNIS, P. J.—STÖVER, D.: J. Mater. Process. Tech., *92–93*, 1999, p. 368. http://dx.doi.org/10.1016/S0924-0136(99)00245-9
[7] PILOUS, V.—STRÁNSKÝ, K.: Strukturní stálost návarů a svarových spojů v energetickém strojírenství. Praha, Academia 1989 (in Czech).
[8] SOPOUŠEK, J.—MILLION, B.: Kovove Mater., *41*, 2003, p. 118.
[9] PAVLOVSKÝ, J.—MILLION, B.—CÍHA, K.—STRÁNSKÝ, K.: Mater. Sci. Eng., *A149*, 1991, p. 105.
[10] PARKER, J.: Int. J. Press. Vessels Pip., *75*, 1998, p. 83. http://dx.doi.org/10.1016/S0308-0161(97)00109-9
[11] PARKER, J. D.—STRATFORD, G. C.: Mater. Sci. Eng., *A299*, 2001, p. 174. http://dx.doi.org/10.1016/S0921-5093(00)01375-7
[12] NICHOLSON, R. D.—WILLIAMS, J. A.: Int. J. Press. Vessels Pip., *20*, 1985, p. 239. http://dx.doi.org/10.1016/0308-0161(85)90056-0
[13] PARKER, J. D.—STRATFORD, G. C.: J. Mater. Sci., *35*, 2000, p. 4099. http://dx.doi.org/10.1023/A:1004846607046
[14] PARKER, J. D.—STRATFORD, G. C.: Mater. Sci. Eng., *A299*, 2001, p. 164. http://dx.doi.org/10.1016/S0921-5093(00)01374-5
[15] WILLIAMS, J. A.—PARKER, J. D.: Mater. Sci. Eng., *A201*, 1995, p. 242. http://dx.doi.org/10.1016/0921-5093(95)09778-3
[16] LAHA, K.—CHANDRAVATHI, K. S.—RAO, K. B. S.—MANNAN, S. L.—SASTRY, D. H.: Metallurgical Mater. Trans., *A32*, 2001, p. 115. http://dx.doi.org/10.1007/s11661-001-0107-9
[17] SIREESHA, M.—ALBERT, S. K.—SUNDARESAN, S.: Int. J. Press. Vessels Pip., *79*, 2002, p. 819. http://dx.doi.org/10.1016/S0308-0161(02)00104-7
[18] LEE, H. Y.—LEE, S. H.—KIM, J. B.—LEE, J. H.: Int. J. Fatigue, *29*, 2007, p. 1868. http://dx.doi.org/10.1016/j.ijfatigue.2007.02.009
[19] CERJAK, H.—MAYR, P.: In: Creep-Resistant Steels. Eds.: Abe, F., Kern, T. U., Viswanathan, R. Cambridge, Woodhead Publishing Ltd. 2008, p. 472. http://dx.doi.org/10.1533/9781845694012.2.472
[20] PARADOWSKA, A. M.—PRICE, J. W. H.—KEREZSI, B.—DAYAWANSA, P.—ZHAO, X. L.: Eng. Fail. Anal., *17*, 2010, p. 320. http://dx.doi.org/10.1016/j.engfailanal.2009.06.016
[21] WANG, H.—ZHANG, H.—LI, J.: J. Mater. Process. Tech., *209*, 2009, p. 2803. http://dx.doi.org/10.1016/j.jmatprotec.2008.06.035
[22] STERJOVSKI, Z.—DUNNE, D. P.—AMBROSE, S.: Int. J. Press. Vessels Pip., *81*, 2004, p. 465. http://dx.doi.org/10.1016/j.ijpvp.2003.12.007
[23] VAILLANT, J. C.—VANDENBERGHE, B.—HAHN, B.—HEUSER, H.—JOCHUM, C.: Int. J. Press. Vessels Pip., *85*, 2008, p. 38. http://dx.doi.org/10.1016/j.ijpvp.2007.06.011
[24] ALBERT, S. K.—MATSUI, M.—WATANABE, T.—HONGO, H.—KUBO, K.—TABUCHI, M.: Int. J. Press. Vessels Pip., *80*, 2003, p. 405. http://dx.doi.org/10.1016/S0308-0161(03)00072-3
[25] ALLEN, D. J.—HARVEY, B.—BRETT, S. J.: Int. J. Press. Vessels Pip., *84*, 2007, p. 104. http://dx.doi.org/10.1016/j.ijpvp.2006.09.010
[26] BRZIAK, P.—HOLÝ, A.—BERNASOVSKÝ, P.: Zváranie – Svařování, *3*, 2007, p. 71 (in Slovak).
[27] FRANCIS, J. A.—MAZUR, W.—BHADESHIA, H. K. D. H.: Mater. Sci. Tech., *22*, 2006, p. 1387. http://dx.doi.org/10.1179/174328406X148778
[28] JANDOVÁ, D.—KASL, J.—KANTA, V.: Mater. High Temp., *23*, 2006, p. 165.
[29] TEZUKA, H.—SAKURAI, T.: Int. J. Press. Vessels Pip., *82*, 2005, p. 165. http://dx.doi.org/10.1016/j.ijpvp.2004.09.001
[30] KIMURA, K.—WATANABE, T.—HONGO, H.—YAMAZAKI, M.—KINUGAWA, J.—IRIE, H.: Quarterly J. Japan Weld. Soc., *21*, 2003, p. 195. http://dx.doi.org/10.2207/qjjws.21.195
[31] MÜSCH, H.—MEYER, H.—REMMERT, H.—SCHLÜTER, N.: VGB Kraftwerkstechnik, *77*, 1997, p. 858.
[32] SKLENIČKA, V.—KUCHAŘOVÁ, K.—KUDRMAN, J.—SVOBODA, M.—KLOC, L.: Kovove Mater., *43*, 2005, p. 20.
[33] HOMOLOVÁ, V.—JANOVEC, J.—KROUPA, A.: Mater. Sci. Eng., *A335*, 2002, p. 290.
[34] HÄTTESTRAND, M.—ANDRÉN, H. O.: Micron, *32*, 2001, p. 789.
[35] SAWADA, K.—BAUER, M.—KAUFFMANN, F.—MAYR, P.—KLENK, A.: Mater. Sci. Eng., *A527*, 2010, p. 1417. http://dx.doi.org/10.1016/j.msea.2009.10.044
[36] ORLOVÁ, A.—BURŠÍK, J.—KUCHAŘOVÁ, K.—SKLENIČKA, V.: Mater. Sci. Eng., *A245*, 1998, p. 39.
[37] MARSHALL, P.: Austenitic Stainless Steels: Microstructure and Mechanical Properties. London and New York, Elsevier Applied Science Publishers 1984.
[38] VACH, M.—KUNÍKOVÁ, T.—DOMÁNKOVÁ, M.—ŠEVC, P.—ČAPLOVIČ, Ľ.—GOGOLA, P.—JANOVEC, J.: Mater. Char., *59*, 2008, p. 1792. http://dx.doi.org/10.1016/j.matchar.2008.04.009
[39] JANOVEC, J.—ŠUŠTARŠIČ, B.—MEDVED, J.—JENKO, M.: Materiali in tehnologije, *37*, 2003, p. 307.
[40] KOZUH, S.—GOJIC, M.—KOSEC, L.: Kovove Mater., *47*, 2009, p. 253.
[41] RAMIREZ, A. J.—LIPPOLD, J. C.: Mater. Sci. Eng., *A380*, 2004, p. 266, p. 269.
[42] JONŠTA, Z.—JONŠTA, P.—VODÁREK, V.—MAZANEC, K.: Acta Metallurgica Slovaca, *13*, 2007, p. 549.
[43] VODÁREK, V.—STŘÍLKOVÁ, L.—KUBOŇ, Z.: In: Proceedings of the 18th International Conference on Metallurgy and Materials METAL 2009 (ISBN 978-80-87294-03-1). Ostrava, TANGER Ltd. 2009.

[44] SOPOUŠEK, J.—BURŠÍK, J.—BROŽ, P.: Intermetallics, *13*, 2005, p. 876.

[45] FUCHS, R.—HEUSER, H.—HAHN, B.: Mater. High Temp., *27*, 2010, p. 189.